Using Eqs. (2.83) and (2.86), we get the following possjbilities for the different quantum numbers, which are displayed in Table 2.2.

According to Eqs. (2.85) and (2.88), the levels with different values of n_z are split for small deformations proportionally to δ. This is shown in Fig. 2.19.

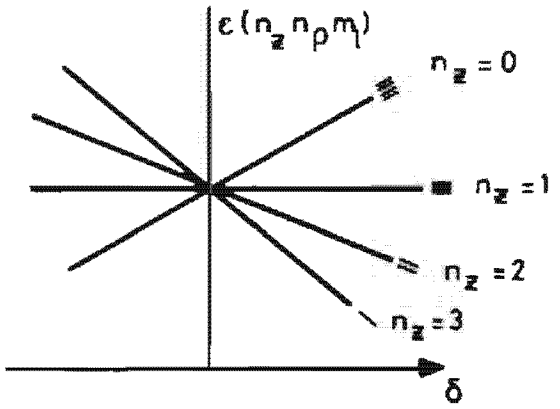

Figure 2.19. Levels of the anisotropic harmonic oscillator as a function of δ.

2.8.4 Nilsson Hamiltonian

As we have seen in Sec. 2.3, the pure harmonic oscillator has two essential drawbacks concerning the agreement with experimental single-particle spectra:

(i) A strong spin orbit term must be added in order to reproduce the right magic numbers
(ii) For heavy nuclei, the realistic average potential is rather flat in the interior of the nucleus. Compared to the harmonic oscillator, nucleons at the surface (i.e., nucleons with higher l-values) feel a deeper potential in the realistic case.

In order to include these effects, Nilsson [Ni 55] added two terms to the deformed harmonic oscillator (2.74) and (2.80) and used the Hamiltonian:

$$h = -\frac{\hbar^2}{2m}\Delta + \frac{m}{2}\omega_\perp^2(x^2+y^2) + \frac{m}{2}\omega_z^2 z^2 + C\mathbf{l}\mathbf{s} + D\mathbf{l}^2 \tag{2.89}$$

$$= \hbar\omega_0(\delta)\left(-\frac{1}{2}\Delta' + \frac{1}{2}r'^2 - \beta r'^2 Y_{20}\right) - \kappa\hbar\omega_0(2\mathbf{l}\mathbf{s} + \mu\mathbf{l}^2). \tag{2.90}$$

The constants C and D are given in the form:

$$C = -2\hbar\omega_0\kappa, \qquad D = -\hbar\omega_0\kappa\mu, \tag{2.91}$$

where C gives the strength of the spin orbit force and $D\cdot\mathbf{l}^2$ shifts the levels with higher l-values downward (Fig. 2.20; notice that different μ-values are taken for different shells, as explained below).

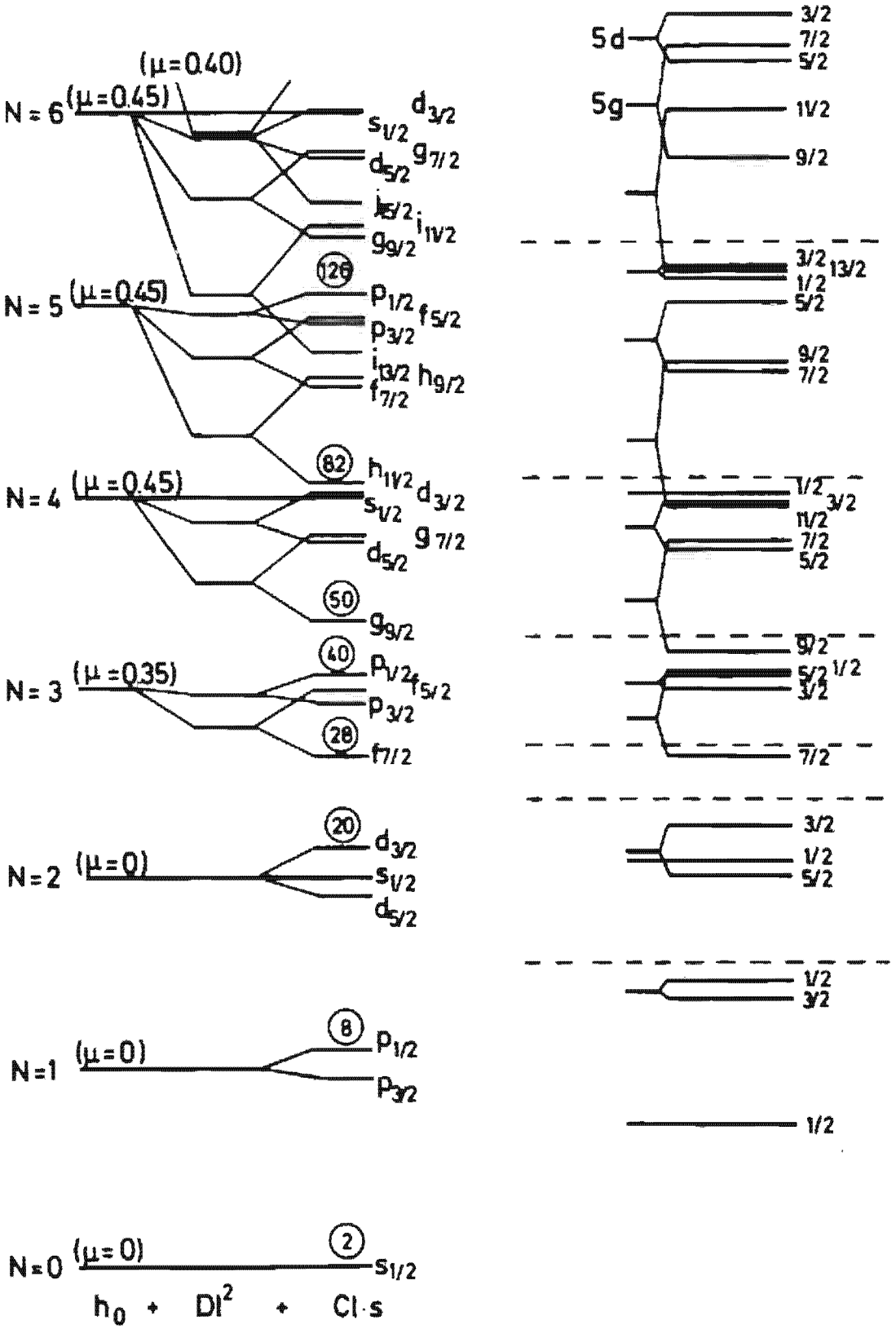

Figure 2.20. Comparison of experimentally determined level scheme [Kl 52] with calculations [Ni 55] using the Nilsson Hamiltonian for zero deformation.

In the original version, Nilsson used the term $D \cdot \mathbf{l}^2$. Later on one observed that for states with large N quantum numbers, the corresponding shift is too strong and the following replacement was made [GLN 67]

$$D \cdot (\mathbf{l}^2 - \langle \mathbf{l}^2 \rangle_N), \tag{2.92}$$

where $\langle \mathbf{l}^2 \rangle_N = \frac{1}{2} \cdot N(N+3)$ is the expectation value of $\mathbf{l}^2$ averaged over one major shell with quantum number N. In this case, only the states within the shells are shifted. The center of gravity between different major shells remains unaffected.

Of course, the $\mathbf{l} \cdot \mathbf{s}$ and the $\mathbf{l}^2$ term are no longer diagonal in the representation $n_z\, n_\rho\, m_l$, nor in the representation n_x, n_y, n_z. The only quantum numbers that remain conserved are the parity π and the eigenvalue Ω of j_z. In fact, it is easily shown that h of Eq. (2.90) does not commute with $\mathbf{J}^2$; therefore the Slater determinant for a deformed shell model has no good quantum number for the total angular momentum. This means that the picture of a deformed nucleus, that is, a deformed shell model, is inevitably linked to the abandonment of rotational invariance. In nature, however, rotational invariance is never violated and one should therefore, at least in principle, re-establish this invariance before drawing any conclusions. How this can be done will be shown in Sec. 11.4. Approximate treatments of these so-called projection methods show that the main features of the deformed shell model are correct.

For large deformations, the $\mathbf{ls}$ and $\mathbf{l}^2$ terms in Eq. (2.90) can be neglected in comparison with βY_{20}. In this limit, the quantum numbers (2.87) of the anisotropic harmonic oscillator become good quantum numbers. They are then also termed *asymptotic quantum numbers*.

In order to obtain the eigenvalues of the Nilsson Hamiltonian as a function of δ, it must be diagonalized in a suitable basis. The isotropic or anisotropic harmonic oscillator [BP 71] can be used as a basis set. In his original paper, Nilsson [Ni 55] worked in a spherical basis. In this case, the $\mathbf{l}^2$ and $\mathbf{ls}$ terms are diagonal and only the term βY_{20} mixes states with the same principal quantum number N ($\Delta N = 0$) with those with $\Delta N = 2$. By using stretched coordinates Nilsson could show [Ni 55] that the $\Delta N = 2$ admixtures are only of higher order in the deformation parameter and can therefore be neglected to a good approximation. The deformation parameters in the stretched coordinates are usually called ϵ_i. Because of the $\mathbf{ls}$ and $\mathbf{l}^2$ terms, the levels with the same n_z in Fig. 2.19 split up and only the degeneracy $\pm\Omega$ is conserved. Nevertheless, the levels with the same n_z are, in the asymptotic region, nearly parallel. This effect can be seen in the so-called Nilsson diagram of Fig. 2.21a, for instance, for the levels with $N = 3$. In Figs. 2.21b and 2.21c the Nilsson diagrams for higher shells are given for neutrons and protons, respectively. Again, we can see that levels with the same n_z are parallel in the asymptotic region. For the correct attribution of the n_z quantum number, one should also notice that according to Eq. (2.85), levels with higher (lower) n_z values are lower than those

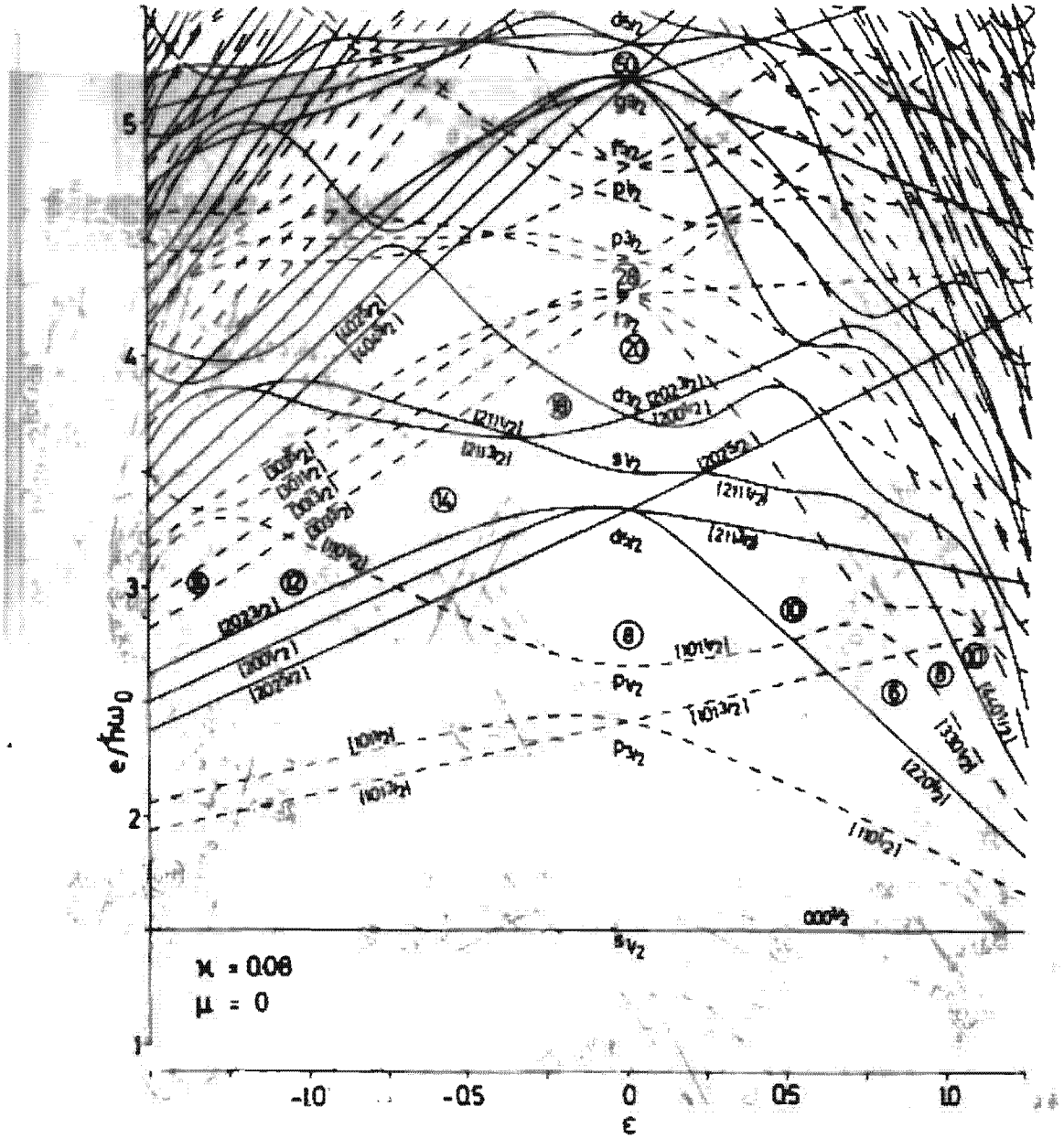

Figure 2.21a. Level scheme of the Nilsson Model for light nuclei. The figure shows the single-particle energies e [the eigenvalues of the Nilsson Hamiltonian (2.90)] in units of the oscillator energy $\hbar\omega_0(\epsilon)$ at the corresponding deformations $\epsilon = \epsilon_2$ (stretched coordinate; see text). The full lines correspond to levels with positive parity, the dashed lines to those with negative parity. The numbers on the lines correspond to the quantum numbers N, n_z, m_l, Ω. Also indicated are the magic numbers in the spherical case and for finite deformations. (We are grateful to Dr. S. Åberg for the preparation of the figure.)

with lower (higher) n_z-values for positive (negative) δ. Knowing N, n_z, and Ω one can also determine the m_l value, and hence the complete set of asymptotic quantum numbers, from tables analogous to Table 2.2.

The Nilsson Hamiltonian (2.90) contains no Coulomb term. The effect of that term is incorporated into an appropriate choice of the constants κ and μ. They are actually fitted such that the observed levels in deformed nuclei are reproduced. The spherical single-particle energies that one obtains with these parameters agree qualitatively with the single-particle or

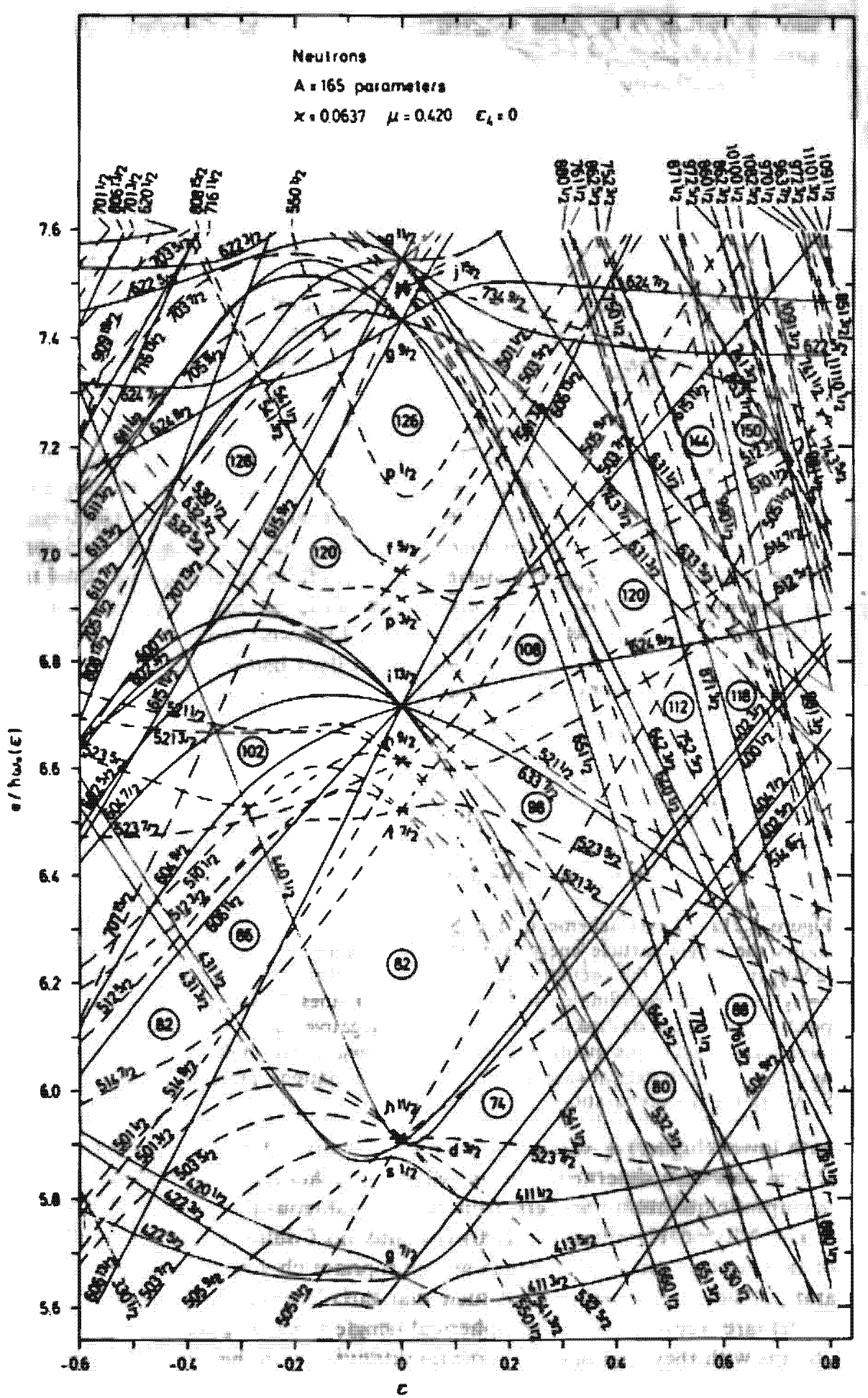

Figure 2.21b. Same as Fig. 2.21a for neutrons in heavy nuclei.

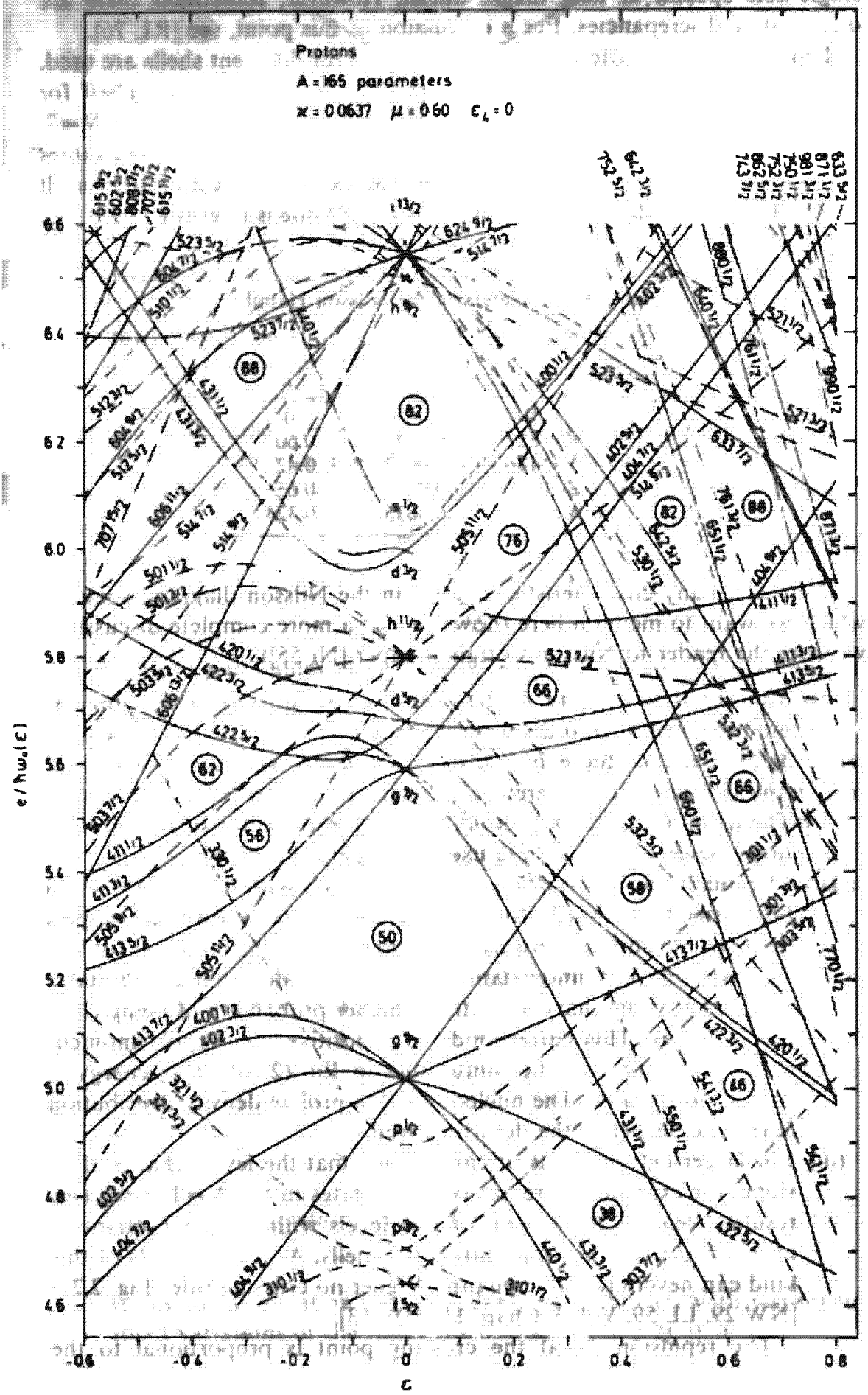

Figure 2.21c. Same as Fig. 2.21a for protons in heavy nuclei.

single-hole spectra of near magic nuclei. However, sometimes there are quantitative discrepancies. For a discussion of this point, see [RL 76].

To get a good fit, different values of κ and μ for different shells are used. In his original paper, Nilsson used $\kappa = 0.05$ for all shells and $\mu = 0$ for $N = 0, 1, 2$; $\mu = 0.35$ for $N = 3$; $\mu = 0.45$ for $n = 4, 5, 6$; and $\mu = 0.4$ for $N = 7$. Later these parameters were more carefully adjusted. Table 2.3 gives values that are now widely used. There the same values of μ and κ are used for all the shells, but they depend on the nucleus (N, Z) one is interested in.

Table 2.3 Parameters of the Nilsson Hamiltonian (from [GLN 67])

Region	κ	μ
$N, Z < 50$	0.08	0
$50 < Z < 82$	0.0637	0.60
$82 < N < 126$	0.0637	0.42
$82 < Z$	0.0577	0.65
$126 < N$	0.0635	0.325

There are many characteristic features in the Nilsson diagram, some of which we want to mention here (however, for a more complete discussion, we refer the reader to Nilsson's original paper [Ni 55]):

(i) The shells which are determined by the single particle angular momentum j at zero deformation, split up into $(2j+1)/2$ levels for $\delta \neq 0$. Each of these is twofold degenerate with eigenvalues $\pm\Omega$ ($[h, j_z] = 0$) and can therefore be characterized by $|\Omega|$ and its parity. The quantum numbers $[Nn_z m_l]$ are not conserved for small deformations, nevertheless they are used to classify the levels.

(ii) The quadrupole field $r'^2 Y_{20}$ causes the levels with lower Ω values to be shifted downwards for positive deformations (prolate shapes) and to be shifted upwards for negative deformations (oblate shapes). One can understand this effect, realizing that the states with low Ω-values have a relatively higher probability of being close to the z-axis. This corresponds to a positive quadrupole moment $\langle r'^2 Y_{20} \rangle$. Because of the minus sign in Eq. (2.90), their energy is shifted downwards. The nucleons with a prolate density distribution $|\phi_i(\mathbf{r})|^2$ lie deeper in the deformed well.

(iii) For larger deformations, it can happen that the levels change their slope, for example, there are two $1/2$-states in the $N = 1$ shell. This results from the interaction of two levels with the same quantum numbers $\Omega\pi$ coming from different j-shells. As a rule, levels of this kind can never cross (Neumann–Wigner no crossing rule; Fig. 2.22) [NW 29, LL 59, Vol. 3, Chap. 11; HW 53].

The repulsion $\Delta\epsilon$ at the crossing point is proportional to the interaction strength. Properties of the levels become interchanged at

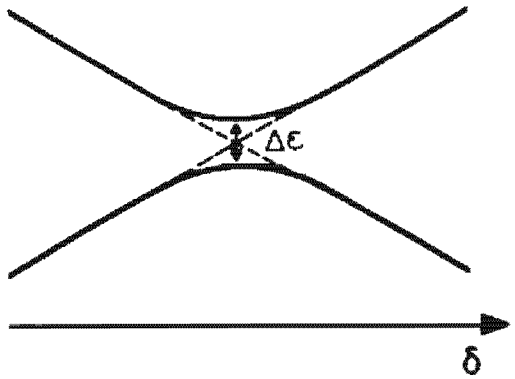

Figure 2.22. No crossing rule for two levels with the same symmetry.

the crossing point and the wave functions corresponding to the two levels far from the crossing point are the same as if there had been no interaction at all.

(iv) If one diagonalizes the Nilsson Hamiltonian using the basis $|Nlj\Omega\rangle$ of the isotropic harmonic oscillator, the Nilsson wave functions are given by a superposition of spherical harmonic oscillator functions:

$$|k\rangle = \sum_{\alpha} D_{\alpha k}|\alpha\rangle, \tag{2.93}$$

where

$$\alpha = \{Nlj\Omega\}.$$

For small values of δ, there is only small mixing, that is, one of the coefficients $D_{\alpha k}$ is nearly equal to one, and the others are close to zero. For larger deformations, the situation depends very much on the specific levels. For example, the $1g_{9/2}$ state in Fig. 2.21c splits up into five levels $\Omega = 1/2, \ldots, 9/2$. Since for $\delta = 0$ the $g_{9/2}$ is rather far away from the other levels with the same N (it is lowered by the spin orbit term), there is only a small amount of mixing, and the corresponding levels are almost eigenstates of $\mathbf{j}^2$, even for quite large values of δ. The same effect is even more pronounced for heavier nuclei. For instance, the $i_{13/2}$ state is of this type and plays an important role in the rare earth region and contains almost no mixing for relevant deformation values.

(v) The slope of the Nilsson levels ϵ_k [measured in units of $\hbar\omega_0(\epsilon)$] is given by the single-particle matrix element of the quadrupole operator $q = r'^2 Y_{20}$ in the corresponding single-particle state $|k\rangle$

$$\frac{d\epsilon_k}{d\beta} = -\langle k|r'^2 Y_{20}|k\rangle.$$

To prove this relation, we use the fact that the eigenvalues

$$\epsilon_k = \langle k|h(\beta = 0) - \beta q|k\rangle$$

of the diagonalization problem (2.90) are stationary with respect to small variations of the functions $|k\rangle$ (see Sect. 5.2), that is,

$$\delta\langle k|h(\beta = 0)|k\rangle - \beta\,\delta\langle k|q|k\rangle = 0.$$

We thus obtain

$$\frac{d\epsilon_k}{d\beta} = \frac{d}{d\beta}\langle k|h(\beta=0)|k\rangle - \beta\frac{d}{d\beta}\langle k|q|k\rangle - \langle k|q|k\rangle = 0 - \langle k|q|k\rangle.$$

2.8.5 Quantum Numbers of the Ground State in Odd Nuclei

The spherical shell model fails in its prediction for the angular momenta and parities of the ground state for nuclei in the deformed region. However, the Nilsson model is able to explain the experimental data in the following way [MN 59].

For a specific nucleus, one determines the deformation parameter δ from the measured quadrupole moment Q_0, as discussed in Section 2.8.1. For this value of δ one successively fills two protons and two neutrons in each level starting from the bottom. Because of the degeneracy of each Nilsson level ($\pm\Omega$), every nucleon pair has, qualitatively speaking, spin zero. Therefore spin and parity of odd nucleons are determined by the last odd nucleon. Since Ω is not a directly measurable quantity, we must determine it indirectly by using a model. We will see in Section 3.3.1.1 that the appropriate concept here is the particle-plus-rotor model. There it will turn out that the angular momentum I_0 of the band head of a rotational band coincides with Ω ($I_0 = \Omega$). The lowest band head is, therefore, the ground state spin of the odd nucleus. Often in the region of the experimentally determined value of δ several possibilities for the Ω of the last particle exist. In fact, the observed value of the ground state spin for many deformed nuclei is among the possible Ω values indicated in Table 2.4. In Fig. 2.23 this method is explained for $^{183}_{74}W_{109}$. The other possible Ω values

Table 2.4 Comparison of theoretically and experimentally determined ground state spins [He 61, p. 648]

	δ	$I_{0\,\text{theo}}$	$I_{0\,\text{exp}}$		δ	$I_{0\,\text{theo}}$	$I_{0\,\text{exp}}$
$_{63}Eu^{151}$	0.16	$3/2^{\pm}, 5/2^{\pm}, 1/2^-$	5/2	Gd^{155}_{91}	0.31	$5/2^+, 3/2^-$	3/2
$_{63}Eu^{153}$	0.30	$5/2^+, 3/2^+$	5/2	Gd^{157}_{93}	0.31	$3/2^-, 5/2^+$	3/2
$_{65}Tb^{159}$	0.31	$3/2^+, 5/2^+$	3/2	Dy^{161}_{95}	0.31	$5/2^-$	
$_{67}Ho^{165}$	0.30	$7/2^-, 1/2^+$	7/2	Er^{167}_{99}	0.29	$1/2^-, 7/2^+, 11/2^-$	7/2
$_{69}Tm^{169}$	0.28	$1/2^+, 7/2^-$	1/2	Yb^{171}_{101}	0.29	$7/2^+, 1/2^-, 11/2^-$	1/2
$_{71}Lu^{175}$	0.28	$7/2^+, 5/2^+$	7/2	Yb^{173}_{103}	0.29	$5/2^-$	5/2
$_{73}Ta^{181}$	0.23	$5/2^+, 7/2^+$	7/2	Hf^{177}_{105}	0.26	$7/2^-$	7/2
$_{75}Re^{183}$	0.19	$9/2^-, (5/2^+)$	5/2	Hf^{179}_{107}	0.27	$9/2^+$	9/2
$_{75}Re^{187}$	0.19	$9/2^-, (5/2^+)$	5/2	W^{183}_{109}	0.21	$1/2^-, 7/2^-, 3/2^-$	1/2
$_{77}Ir^{191}$	0.14	$3/2^+, 1/2^+, 11/2^-$	3/2	Os^{187}_{111}	0.18	$1/2^-, 3/2^-, 9/2^-$	1/2
$_{77}Ir^{193}$	0.12	$3/2^+, 1/2^+, 11/2^-$	3/2	Os^{189}_{113}	0.15	$1/2^-, 3/2^-, 11/2^+, (9/2^-)$	3/2

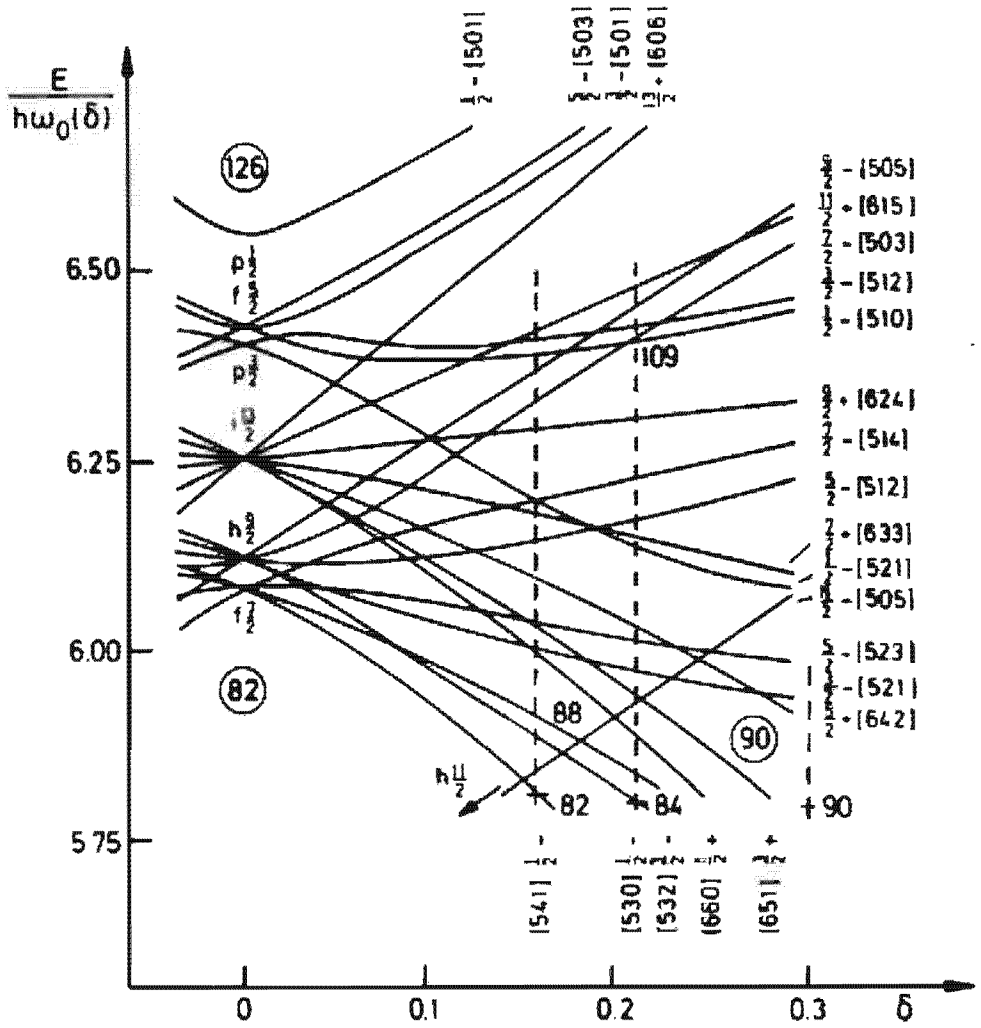

Figure 2.23. Determination of the ground state spin in the Nilsson model. (From[He 61, p. 647].)

are usually seen in the spectra as band heads of excited rotational bands, which is a nice success of the Nilsson model. Single-particle energies in this scheme can be found in [Ch 66, BR 71a, OWP 71, GIS 73, GSK 75, CAF 77].

2.8.6 Calculation of Deformation Energies

In order to obtain the ground state energy of the nucleus in the (spherical or deformed) shell model, we cannot simply sum the single-particle energies from the bottom of the potential up to the Fermi level, because the effect of the nucleon–nucleon interaction would be counted twice (see also Sec. 5.3). To account for this, we proceed with the following qualitative considerations.

We assume that the average potential which is felt by the ith nucleon is given by the sum of all two-body potentials acting on this particle:

$$V_i = \sum_{j \neq i} v_{ij}. \tag{2.94}$$

The Hamilton operator

$$H = \sum_{i=1}^{A} t_i + \tfrac{1}{2} \sum_{\substack{i,j \\ i \neq j}} v_{ij} \tag{2.95}$$

is then given by

$$H = \tfrac{1}{2} \sum_{i=1}^{A} h_i + \tfrac{1}{2} \sum_{i=1}^{A} t_i; \qquad h_i = t_i + V_i. \tag{2.96}$$

If V_i has the form of a harmonic oscillator, we have, because of the virial theorem [Da 65a, Chap. II],

$$\langle t_i \rangle = \langle V_i \rangle = \tfrac{1}{2} \langle h_i \rangle \tag{2.97}$$

and we get as the ground state energy

$$E_0(\delta) = \langle H \rangle = \tfrac{3}{4} \sum_{i=1}^{A} \langle h_i \rangle = \tfrac{3}{4} \sum_{i=1}^{A} \epsilon_i(\delta). \tag{2.98}$$

In practice we determine the equilibrium deformation δ_{eq} in calculating E_0 as a function of δ; the absolute minimum then determines δ_{eq}. This procedure does not, of course, include any residual interaction and, in fact, fails to reproduce the absolute value of the binding energies. Only the resulting equilibrium deformations are approximately right (see Fig. 2.24). Further investigations on these lines [BS 61, Sz 61, So 67, and GLN 67] have taken into account the following additional points.

(i) A *residual interaction* of the pairing type (see Chap. 6)
(ii) The expectation value of the *Coulomb force*

$$E_{\text{Coul}} = \Big\langle \sum_{\text{prot}} \frac{e^2}{|\mathbf{r}_i - \mathbf{r}_j|} - \kappa \hbar \omega_0 \Delta\mu \sum_{\text{prot}} \left(\mathbf{l}^2 - \langle \mathbf{l}^2 \rangle_N \right) \Big\rangle, \tag{2.99}$$

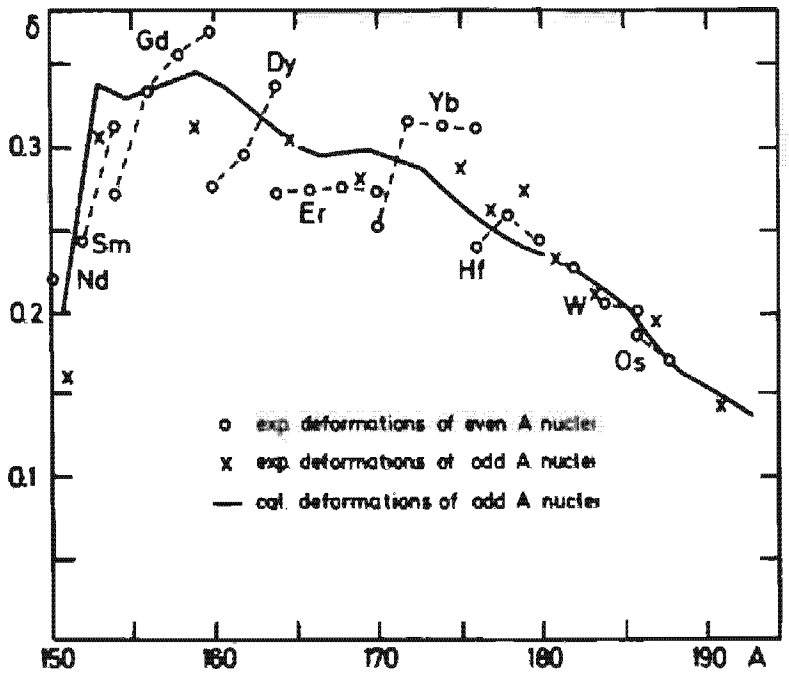

Figure 2.24. Comparison of theoretically and experimentally determined deformations. (From [MN 55].)

where $\Delta\mu = \mu_{prot} - \mu_{neut}$ corrects for the Coulomb effect already taken into account by the difference between the proton and neutron parameters μ. It turns out that the effect of the Coulomb repulsion favors larger deformations, whereas the effect of the pairing correlations is the converse. On the whole, the results of the old Nilsson model are reproduced, because Coulomb and pairing forces counteract one another at the equilibrium point.

(iii) *Higher shapes*. It is evident that quadrupole deformations alone are not able to describe for instance the fission process. On the other hand, there exists evidence for hexadecupole deformations in the ground state of some nuclei [HGH 68]. It is possible to describe such effects within the Nilsson model by including, besides Y_{20}, higher terms such as Y_{40} and Y_{60} [NTS 69, Mö 72, MN 73, RNS 78].

For the fission process it is often useful to introduce deformed potentials that allow us to describe two separated fragments at large distances. In contrast to the Nilsson model, such potentials have the right asymptotic behavior. Several versions of such potentials have been used:

(i) *Two-center models* [DR 66, HMG 69, ADD 70, GMG 71, SGM 71, MG 72, MMS 73], which are based on two oscillators with separated centers.

(ii) The *Folded Yukawa Potential* [Ni 69, BFN 72, Ni 72, MN 73] which starts with a density of sharp surface but arbitrary shape. To get the corresponding potential, it is folded with a short-range Yukawa force.

(iii) *Generalized Wood–Saxon* potentials with a deformation-dependent surface thickness [DPP 69, BDJ 72, Pa 73, BLP 74, JH 77].

The method of simply summing up the single-particle energies fails to reproduce the absolute binding energies and to describe the energy surface at very large distortions. The reason for this is that the binding energy is a bulk property. In fact, rather small shifts in the single-particle energies produce large errors in the binding energy. To get the proper values for the binding energy together with shell effects, we must use a combination of the liquid drop and the shell model, as proposed by Strutinski (see Sec. 2.9). Calculations within this method show that the pure shell model as described in this chapter allows us to determine only ground state deformations.

The fact that the absolute energy minimum occurs at finite values of δ for nuclei between closed shells, can be understood qualitatively by considering the level density as a function of deformation. It turns out that for quite general average potentials the level density develops shell effects for certain definite values of the deformation; that is, at these deformations the levels are not randomly distributed as a first glance on the Nilsson

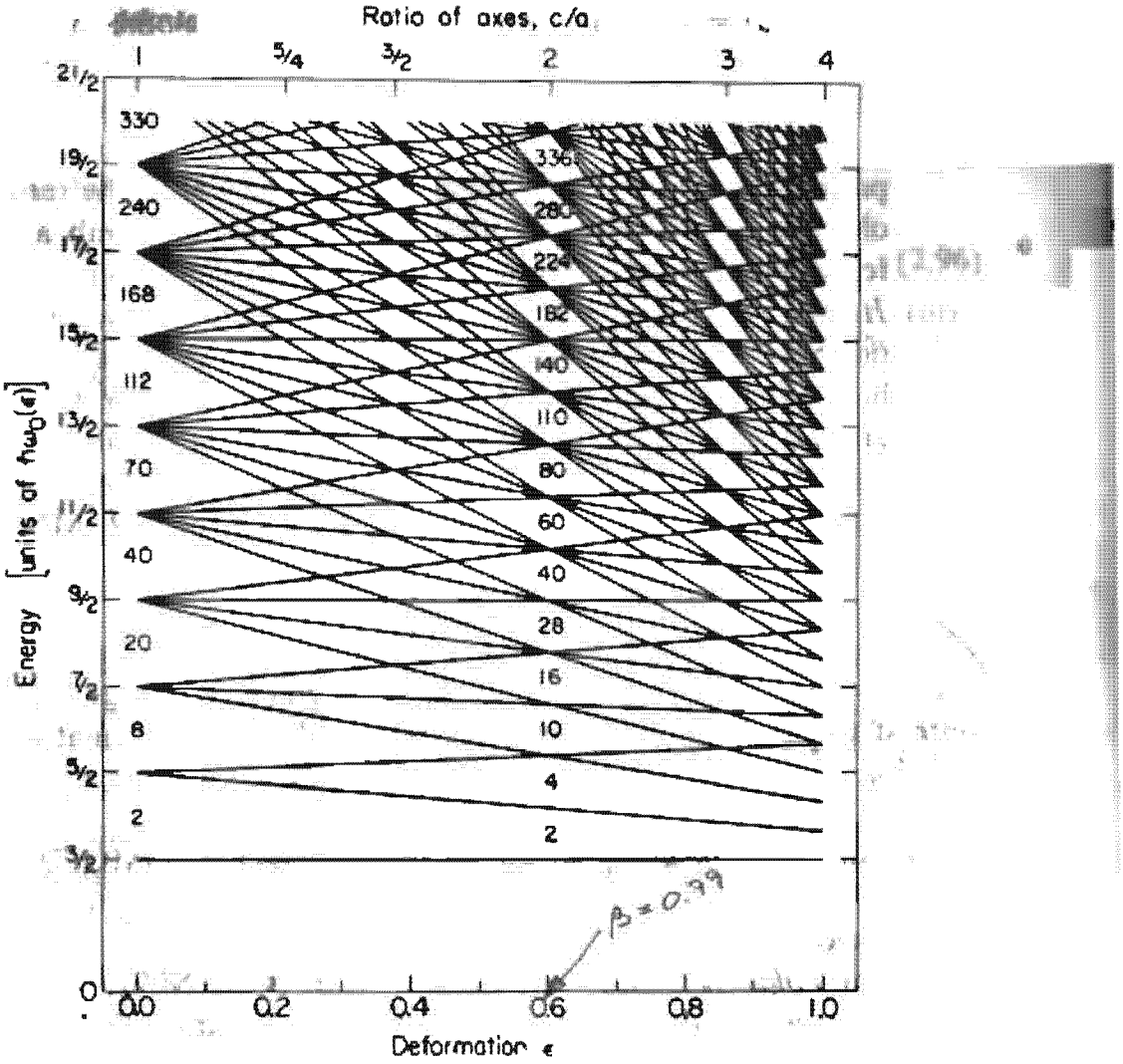

Figure 2.25. Energy levels of an harmonic-oscillator potential for prolate spheroidal deformations ϵ. (From [MN 73].)

diagram would indicate, but are, for instance, grouped in bunches at larger deformations.* This is shown in Fig. (2.25) for the harmonic oscillator.

If one plots the energy as a function of the deformation, one finds that whenever the Fermi level is situated in a low density region, the nucleus is more bound, whereas it is less bound when the Fermi level is in a high density region. This, in turn, means that the occupied levels are, on the average, more bound if the Fermi level is in a low density region than if it is in a high density region. Since for nuclei between closed shells the Fermi level for $\delta = 0$ is in a region of high level density, it becomes qualitatively understandable that these nuclei want to deform into a region where the Fermi energy is in a lower level density region. From this it also becomes clear that in any nucleus more than one minimum, as a function of deformation, can eventually develop. As we discussed in Section 2.8.2, in very heavy nuclei we find second minima at about $\delta \simeq 0.6$, somewhat

*One can understand from semiclassical arguments, at which deformations such shell closures have to occur [BM 75, St 75b, SM 76, SMO 77].

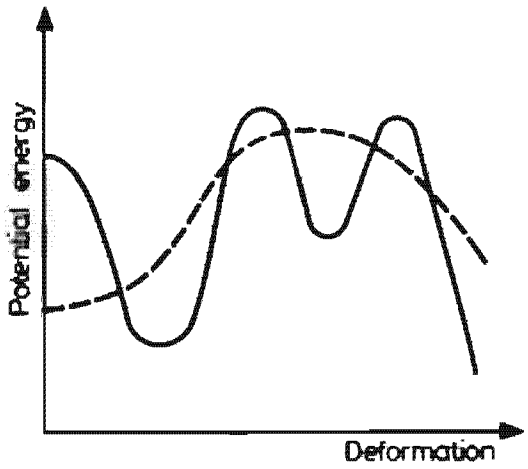

Figure 2.26. Schematic variation of the energy with deformation for a nucleus with a second minimum. The dashed line corresponds to the liquid drop barrier.

higher than the first minimum, which gives rise to the so-called shape isomeric states [St 66]. Qualitatively, the energy as a function of deformation is shown in Fig. 2.26.

2.9 Shell Corrections to the Liquid Drop Model and the Strutinski Method

2.9.1 Introduction

Up to now we have studied two quite different descriptions of the atomic nucleus. The *liquid drop model* (LDM) assumes that the nucleons produce a spatially uniform density distribution in the nucleus with a sharp edge at the surface. It is able to reproduce the overall features of the nucleus, that is, most properties that depend only in a smooth way on the nucleon number, as, for example, in Chapter 1, the A dependence of the nuclear binding energy (Fig. 1.2). On the other hand, there is the *shell model*. It assumes a quantized independent particle motion in an average potential to be valid, and we have seen in Section 2.3 and 2.8 that this model reproduces nicely those particular nuclear properties in which only the nucleons in the vicinity of the Fermi surface are involved.

Phenomenological shell models (in contrast to Hartree–Fock calculations; see Chap. 5), however, fail to correctly reproduce properties of the nucleus in which *all* nucleons contribute (the so-called bulk properties), like, for instance, the total binding energy. Strutinski [St 67, 68] invented a very elegant method* to reconcile both phenomenological descriptions of the nucleus which eliminates their defects but keeps their qualities. This is the *Strutinski shell correction procedure*. It is able to reproduce not only the

* Investigations on a similar line have been carried out by Myers and Swiatecki [MS 66].